

## Computational prediction of the refinement of oxide agglomerates in a physical conditioning process for molten aluminium alloy

This content has been downloaded from IOPscience. Please scroll down to see the full text.

2015 IOP Conf. Ser.: Mater. Sci. Eng. 84 012092

(<http://iopscience.iop.org/1757-899X/84/1/012092>)

View [the table of contents for this issue](#), or go to the [journal homepage](#) for more

Download details:

IP Address: 134.83.1.242

This content was downloaded on 13/08/2015 at 07:57

Please note that [terms and conditions apply](#).

# Computational prediction of the refinement of oxide agglomerates in a physical conditioning process for molten aluminium alloy

M Tong<sup>1</sup>, S C Jagarlapudi<sup>1</sup>, J B Patel<sup>2</sup>, I C Stone<sup>2</sup>, Z Fan<sup>2</sup> and D J Browne<sup>1</sup>

<sup>1</sup>School of Mechanical and Materials Engineering, University College Dublin, Belfield, Dublin 4, Ireland

<sup>2</sup>Brunel Centre for Advanced Solidification Technology, Brunel University, Uxbridge, Middlesex, UB8 3PH, UK

E-mail: Mingming.tong@ucd.ie

**Abstract** Physically conditioning molten scrap aluminium alloys using high shear processing (HSP) was recently found to be a promising technology for purification of contaminated alloys. HSP refines the solid oxide agglomerates in molten alloys, so that they can act as sites for the nucleation of Fe-rich intermetallic phases which can subsequently be removed by the downstream de-drossing process. In this paper, a computational modelling for predicting the evolution of size of oxide clusters during HSP is presented. We used CFD to predict the macroscopic flow features of the melt, and the resultant field predictions of temperature and melt shear rate were transferred to a population balance model (PBM) as its key inputs. The PBM is a macroscopic model that formulates the microscopic agglomeration and breakage of a population of a dispersed phase. Although it has been widely used to study conventional de-oxidation of liquid metal, this is the first time that PBM has been used to simulate the melt conditioning process within a rotor/stator HSP device. We employed a method which discretizes the continuous profile of size of the dispersed phase into a collection of discrete bins of size, to solve the governing population balance equation for the size of agglomerates. A finite volume method was used to solve the continuity equation, the energy equation and the momentum equation. The overall computation was implemented mainly using the FLUENT module of ANSYS. The simulations showed that there is a relatively high melt shear rate between the stator and sweeping tips of the rotor blades. This high shear rate leads directly to significant fragmentation of the initially large oxide aggregates. Because the process of agglomeration is significantly slower than the breakage processes at the beginning of HSP, the mean size of oxide clusters decreases very rapidly. As the process of agglomeration gradually balances the process of breakage, the mean size of oxide clusters converges to a steady value. The model enables formulation of the quantitative relationship between the macroscopic flow features of liquid metal and the change of size of dispersed oxide clusters, during HSP. It predicted the variation in size of the dispersed phase with operational parameters (including the geometry and, particularly, the speed of the rotor), which is of direct use to experimentalists optimising the design of the HSP device and its implementation.



## 1. Introduction

Significant reductions in energy, production costs and carbon footprint can be achieved by manufacture of high performance automotive components with recycled aluminium alloys instead of primary aluminium alloys. Because scrap aluminium alloys are normally contaminated by harmful elements such as iron, at relatively high levels, a key challenge to the recycling process is the purification of materials. Physically conditioning molten scrap aluminium alloys using high shear processing (HSP) was recently found to be a promising technology for this type of purification. Research at Brunel University [1-6] showed that HSP can refine the solid oxide clusters in molten alloys significantly. These act as effective sites for the nucleation of Fe-rich intermetallic phases. The solidified intermetallic particles can subsequently be removed by the downstream de-drossing process, and hence purify the secondary aluminium alloys by removing the harmful elements (e.g. Fe). Due to the high temperature, opacity of the melt, and the close-coupling feature of the rotor-stator mixing head, it is very difficult to measure the temperature and particularly shear rate of melt inside, and in the close vicinity of the mixing head, without disturbance. Moreover, the shear rate characteristic of laminar melt flow and that of turbulent flow are mathematically formulated in totally different ways. Because the status of fluid flow (e.g. laminar or turbulent) directly depends on operational parameters, it is not easy to experimentally determine the characteristic melt shear rate in the process of HSP. Computational simulation is therefore needed to study the key parameters of the HSP process. By using appropriate mathematical equations that describe the related governing physical mechanisms, and corresponding numerical solution schemes, it is possible to predict computationally a variety of key parameters that are normally difficult to measure experimentally. Moreover, since the input data for such a computer model come from operational parameters and materials' properties that are typical of the HSP process in practice, computational simulation can be used to directly determine the influence of operational parameters on the performance of HSP. The Population balance model (PBM) is a macroscopic model that can formulate the microscopic breakage and agglomeration of a population of a phase that is dispersed in a continuous phase [7-13]. In this paper, we present our PBM modeling of the behaviour of the oxide clusters during HSP.

## 2. Model details

The key governing equation of PBM is the population balance equation (PBE):

$$\frac{\partial f(v,t)}{\partial t} + \nabla \cdot [\vec{V} f(v,t)] = S(v,t) \quad (1)$$

where  $f$  is the number density of dispersed phase (i.e. solid oxide clusters in the case of conditioning molten scrap aluminium alloys with HSP) with internal coordinate  $v$  (the volume of dispersed phase). By using the number density, we can directly plot the size distribution of the dispersed phase and mathematically calculate the mean size.  $\vec{V}$  is the advection velocity of the dispersed phase.  $S$  is the net rate of generation of dispersed phase. We are neglecting, for now, the mechanism of growth and only taking the mechanisms of breakage and agglomeration into account.

Determining the advection velocity of the dispersed phase depends on CFD modelling of melt-solid particle two-phase flow. In the CFD modelling, we use an Eulerian method to formulate the governing continuity, momentum and energy equations for every phase, taking the volume fraction of each phase and the interaction between one phase and another into account.

Once the advection velocity is calculated by the CFD model, the evolution of number density of dispersed phase becomes dependent on the net generation rate in the PBM. In the HSP process, dilute oxide clusters are dispersed in the continuum melt. This mixture is strongly stirred by the mixing head with a rotor-stator design, at a relatively high temperature (e.g. 645 °C in [2]). The mechanisms of fragmentation and agglomeration dominate the change of number density of oxide clusters. Therefore, the net generation rate  $S$  becomes:

$$S(v) = S^+(v) - S^-(v), \quad (2)$$

where  $S^+$  is the birth rate and  $S^-$  is the death rate of oxide clusters due to breakage and agglomeration, respectively, and they follow:

$$S^-(v) = b(v)f(v) + \int_0^\infty a(v, v')f(v, t)f(v', t)dv', \quad (3)$$

$$S^+(v) = \int_v^\infty v'b(v')P(v', v)f(v', t)dv' + \frac{1}{2} \int_0^v a(v-v', v')f(v-v', t)f(v', t)dv', \quad (4)$$

where  $a$  is the agglomeration rate,  $b$  is the breakage rate, and  $P$  is the daughter size distribution function for the breakage. It can be seen that the whole PBM modelling is reduced to determining the value of these 3 terms. The first terms of Eq.3 and Eq.4 represent the contribution of mechanism of fragmentation to the change of number density of oxide clusters, while the second terms of Eq.3 and Eq.4 denote the contribution of mechanism of agglomeration to the change of number density of oxide clusters.

In the sub-model for breakage, the shear rate is the dominant factor. The type of melt flow (i.e. laminar or turbulent) and size of oxide clusters (compared with the Kolmogorov length scale) commonly determine the mathematical formulation of the breakage rate [7-10]. For example, the characteristic shear rate depends on the fact that the melt flow falls in the laminar regime or turbulent regime. In the turbulent regime, the mechanism of fragmentation of oxide clusters depends on if the size of oxide clusters is larger than the size of smallest eddies. In the sub-model for the rate of agglomeration, we consider the mechanism of Brownian motion, differential sedimentation, and shear-induced collision of the dispersed phase [7-10].

We use a discrete method to solve Eq.1. The originally continuous profile of size of oxide clusters is firstly discretized into a collection of discrete size bins and Eq.1 is integrated over each bin and then the discrete form of Eq.1 is solved numerically. The discrete oxide cluster size bins follow a geometrical series and the advection velocity of oxides is input from CFD modelling.

### 3. Configuration of the case study and results of simulation

The case study used in our research is a 2D one. The overall setup of this 2D case study is a very close mimic of the realistic rotor-stator mixer that we are using in experiments. Figure 1 illustrates the geometry of the domain of our 2D case study. This case study corresponds to an infinitely long cylindrical crucible full of molten recycled aluminium alloy, which includes alloy melt and solid oxide clusters. An infinitely long mixing head (with rotor-stator design) is placed at the centre of the crucible to shear the mixture. The impeller of the rotor has 4 flat blades and the cylindrical stator has holes along its circumference. Among the geometrical parameters, the key parameters include the size of the gap between the tip of impeller blades and the internal wall of the stator and the size (and number) of holes in the stator. The diameter of the crucible is 300 mm.

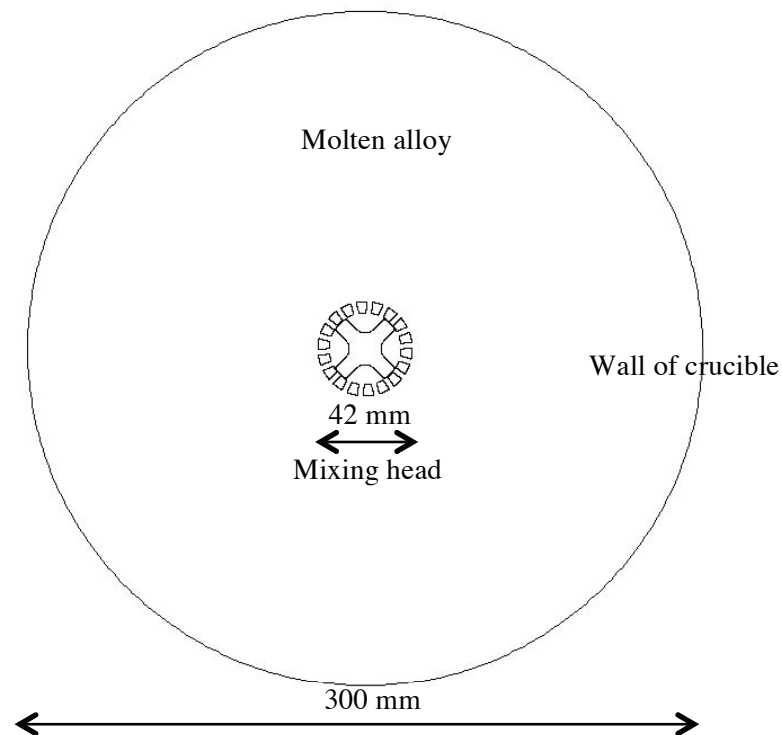


**Figure 1.** Geometrical setup of a 2D case as base line.

In the design of Fig.1, the width of gap between the internal wall of the stator and the tips of impeller blades is 0.25 mm and there are 18 holes of 2.5 mm in diameter each drilled through the stator. The typical operational rotor speed is 5000 rpm. These 3 values, as well as other geometrical features, exactly follow the real situation of the HSP applied in the laboratory, and we are using this setup as the base line case of our simulation.

At the start of simulation, the melt and oxide clusters are set at  $800^{\circ}\text{C}$ , and the size of oxide clusters are assumed to be mono-dispersed with Sauter mean diameter (SMD) of  $10.2\mu\text{m}$ . At the beginning of HSP, the melt/oxide mixture is stationary and the impeller spins at the designated constant rpm. The overall computation is implemented mainly using the FLUENT module of ANSYS. The CFD solver of FLUENT is used to predict the macroscopic flow features of the melt and oxide clusters, including the heat, mass and momentum transfer, using an Eulerian method. The resultant field predictions are transferred to PBM as its key inputs. Although there are some sub-models for the breakage and agglomeration of dispersed phase available in FLUENT, they are mostly suitable for liquid droplets and gas bubbles rather than solid particles. We program our own user subroutines in C for the breakage/agglomeration rates and load them into the PBM solver of FLUENT, in order to run PBM computation.

#### 4. Results of the base line

We set 5 points in the simulation domain, in order to monitor the evolution of parameters of interest. Points 1-3 are located along the axis of a hole in the stator and Points 4 and 5 are in the middle of the far field and near the wall of the crucible, respectively, as shown in Fig.2.

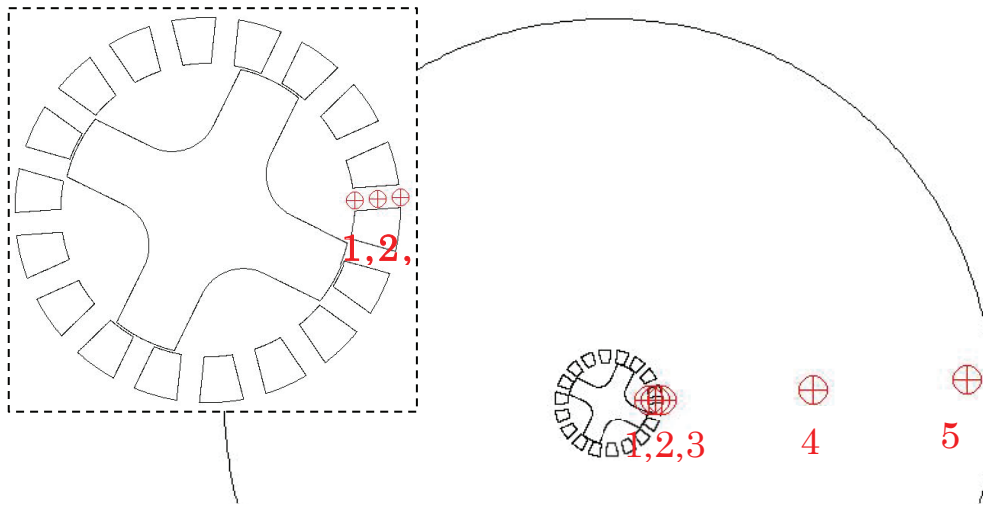


**Figure 2.** Position of sampling points.

If we plot the predicted temporal evolution of SMD of oxide clusters, as in Fig.3, we can find some interesting phenomena. Firstly as shown by the red curve in Fig.3, at the internal orifice of the hole through the stator, the size of oxide clusters drops very dramatically at the start of HSP and then periodically oscillates towards a plateau value. The period of this oscillation is roughly 0.003 s, which is 1/4 the period of impeller spinning. Considering the 4 fold symmetry of the impeller, this is a good agreement.

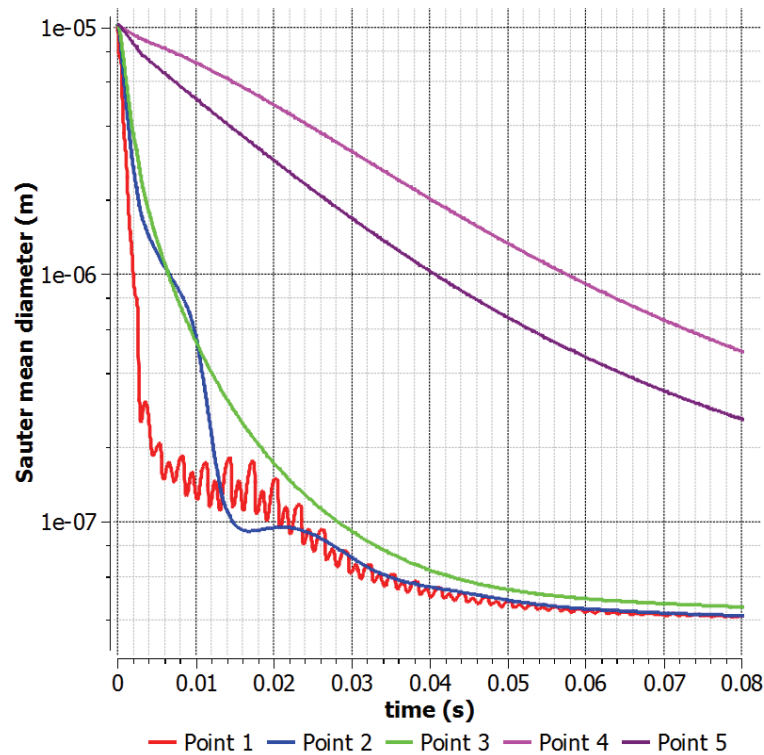


**Figure 3.** Temporal evolution of SMD of oxide clusters at different sampling positions during HSP in the baseline case.

While checking the size of oxide clusters away from the centre of the impeller, over sampling points 2-5, we can find that the size decreases more and more slowly, particularly beyond the rotor.

In order to explain the reason for the significantly different rate of decrease of cluster size at different positions, we plot the contours of some relevant parameters. In this paper, when plotting parameters at a specific moment of time, we use the data when the diameter of oxide clusters sampled at Point 1 has already reached its plateau value (i.e. 0.08 s).

The spatial distribution of oxide cluster size is illustrated in Fig.4. It shows that the spatial distribution is very non-uniform. In the close vicinity of the mixing head, the oxide clusters are as small as  $0.0406\mu\text{m}$ . In the middle of the far field, the oxide clusters are as large as  $0.491\mu\text{m}$ . They are both much lower than the initial oxide cluster size of  $10.2\mu\text{m}$ .

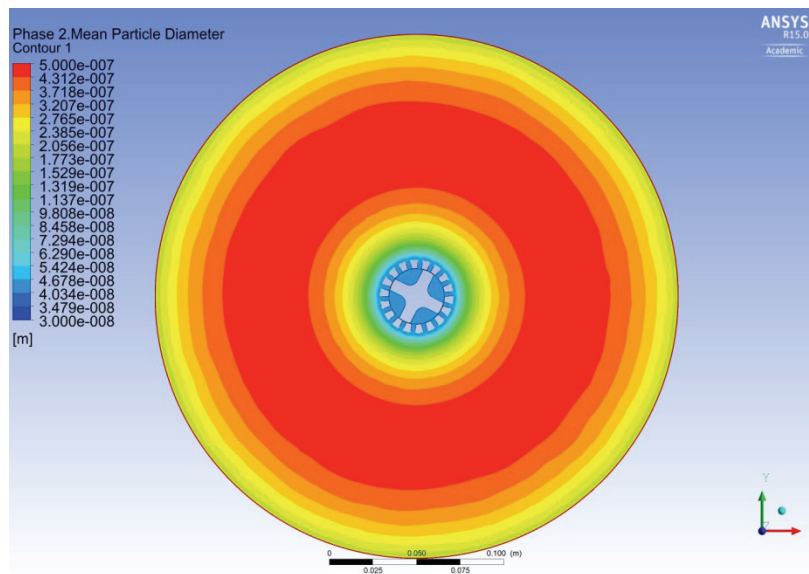


**Figure 4.** Contour of SMD of oxide clusters in the base line case study at 0.08 s.

Figure 5a shows that, in the far field, the fluid flow is highly turbulent and the turbulence becomes relatively less significant in the close vicinity of the mixing head (Fig.5b). However, the value of turbulent viscosity ratio is generally above 30, except inside the very thin boundary layer at the surface of the solid walls of rotor and stator. This means that the shear induced breakage and agglomeration falls into the turbulent regime. The characteristic shear rate of turbulent flow is dominated by the turbulence dissipation rate as:

$$G = \left(\frac{\varepsilon_c}{\nu_c}\right)^{1/2}, \quad (5)$$

where  $G$  is the characteristic shear rate,  $\varepsilon$  and  $\nu$  are the turbulent energy dissipation rate and kinematic viscosity of the melt phase, respectively.

Figure 5 (c,d) demonstrate that the turbulence dissipation rate in the close vicinity of the mixing head is significantly higher than that in the far field, by more than a few orders of magnitude. This makes the breakage and agglomeration of oxide clusters in the close vicinity of the mixing head dramatically stronger than that in the far field. The mechanisms of breakage and agglomeration compete with one another, and the net result is a significant refinement of oxide clusters in the overall crucible by HSP in this 2D case. The particle size at sampling point 4 is larger than that at point 5, as shown in Fig.3. This is because there is a narrow circular band of fluid of slightly lower turbulence dissipation rate, which sweeps right through point 4 as shown in Fig.5c. Such relatively low turbulence dissipation rate directly leads to relatively low characteristic shear rate (Eq.5) and hence relatively large size of oxide

clusters sampled at point 4. While checking the turbulence dissipation rate of fluid from the mixing head towards the wall of crucible along the radial direction of impeller, although the overall trend of the change of its value is decreasing, the decrease does not have to be monotonic. There can be a few radial positions where the value of turbulence dissipation rate is slightly lower than those at their radially neighboring positions, as separately found by Soos et.al. [14] for example. The number and position of such “cold spots” of turbulence dissipation rate of fluid (along the radial direction in the far field) depends on the agitation of the fluid by the impeller and the interaction between the impeller, stator and wall of the crucible.

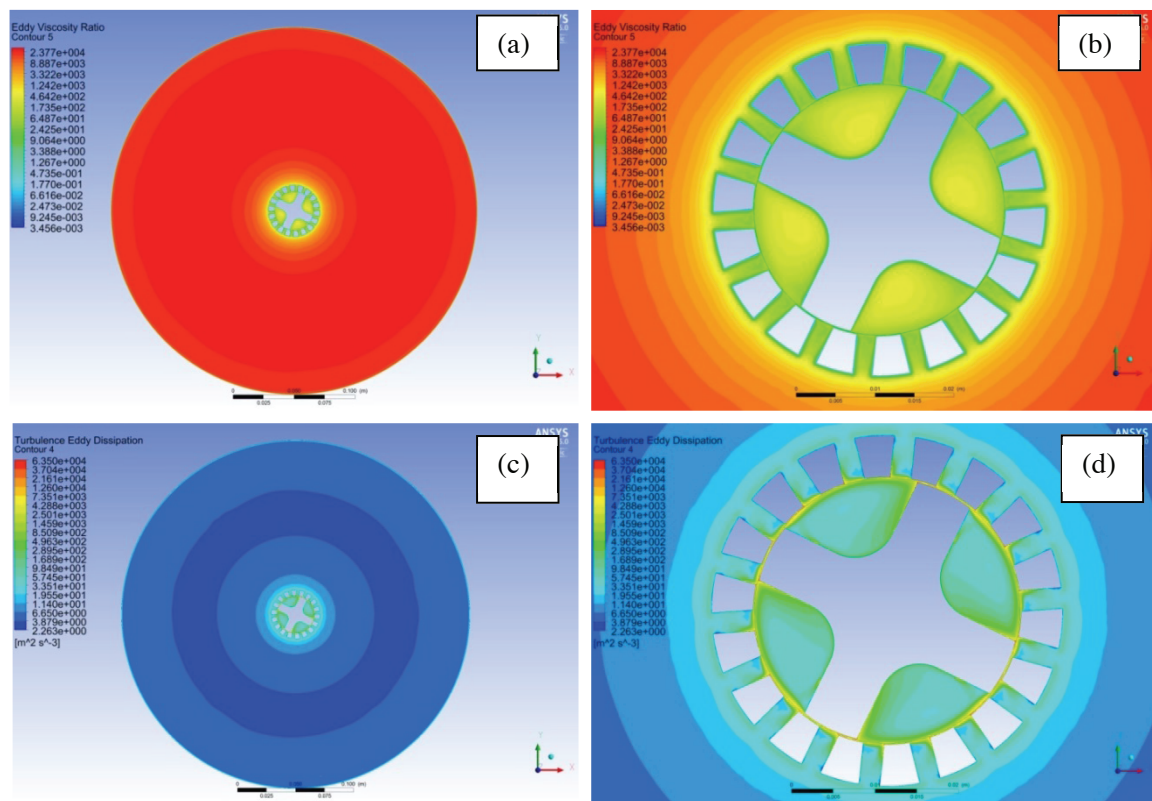


**Figure 5.** Contour of turbulent viscosity ratio of the melt (a), its local zooming in around the mixing head (b), contour of turbulence dissipation rate of melt (c) and its local zooming in around the mixing head (d) in the base line case study at 0.08 s.

Because the fluid in the close vicinity of the mixing head has been found to have the highest level of characteristic shear rate (in both the 2D simulation of this paper and a separate set of 3D case studies of us), we are paying most of our attention to the breakage of oxide clusters in the close vicinity of the mixing head rather than in the far field. The fluid flow in the far field for sure has significant influence on the macroscopic redistribution of fluid and oxide clusters, but it is our major interest in some other separate publication.

### Changing the impeller speed and the geometrical design of the mixing head

In order to investigate the influence of operational rotor speed and geometrical design of the mixing head on the performance of HSP, three different simulations were run, each using a different setup to the reference case study. The rotor speed was reduced from 5000 rpm to 1000 rpm. The size of the gap between the rotor and the stator was increased from 0.25 mm to 2.5 mm. Finally, the number of holes along the circumference of the stator was reduced from 18 to 3, but their diameter was increased from

2.5 mm to 18 mm. Other aspects of the setup of these 3 different cases are as close to those of the base line case as possible. We summarize the simulation results of these 3 different cases and compare them with the result of the base line case, and plot the temporal evolution of oxide cluster size at sampling Point 1, in Fig.6.

Although the size of oxide clusters in the 2.5 mm gap case and the 3 holes case decreases more quickly than the corresponding process of the base line case, the size converges quickly in all of these 3 cases to almost the same plateau value. In the case of running HSP at 1000 rpm, the decrease in size of oxide clusters is significantly slower than the process of base line case and it looks very difficult for the size to converge to the same plateau value as that of the base line case.

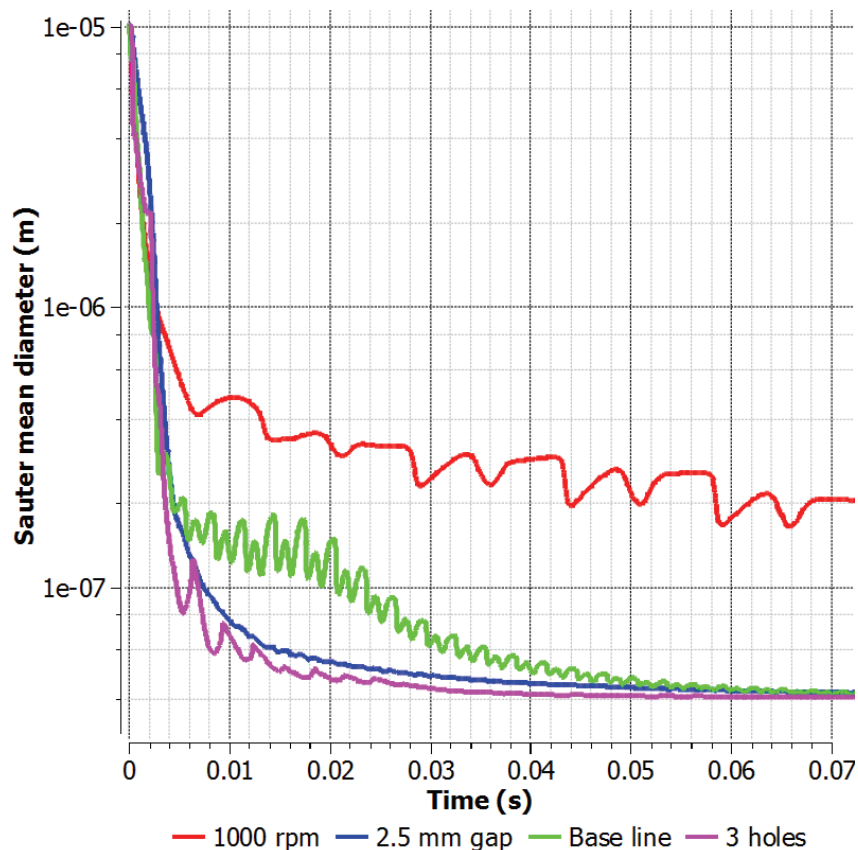


**Figure 6.** Temporal evolution of oxide cluster size sampled at point 1 with different setups.

## 5. Analysis and conclusion

Reviewing the simulation results, in conjunction with the mathematical governing equations, a few interesting conclusions can be drawn. Firstly, the turbulence dissipation rate (and hence characteristic shear rate of turbulent flow) in the 2D HSP case is highly non-uniform in space. Therefore, the resultant refinement of oxide clusters is very non-uniform in space accordingly. Most of the significant refinement of oxide clusters is taking place between the rotor and the stator. This means that a reasonably strong macroscopic redistribution of the molten alloy is necessary if we want to refine all the oxide clusters throughout the whole crucible.

Secondly, after changing related operational and geometrical parameters of the case study and comparing the results against the base line case, we have found a very strong influence of impeller speed on the decrease of oxide cluster size. Although in one case the size of the gap between rotor and

stator was increased to 2.5 mm, which is 10 times that in the base line case, and in a separate case the size of holes was increased to 15 mm in diameter which is 6 times that in the base line case, the temporal evolution of size of oxide clusters sampled at the internal orifice of the holes of the stator quickly converged to an almost common plateau value in all of these 3 cases. However, when we decreased the rotor speed from 5000 to 1000 rpm, it was found that the decrease in size of oxide clusters becomes significantly slower than the corresponding process in the base line case.

Turbulence dissipation rate is the rate at which turbulent kinetic energy is converted into thermal energy due to the viscosity of a fluid. In Fig.5, we can find that the most significant dissipation of turbulent kinetic energy occurs inside the gap between the tips of the impeller blades and the internal wall of the stator. The value of turbulence dissipation here is higher than anywhere else in the computational domain by a few orders of magnitude. This is true even in the case when there are only 3 relative large holes in the stator (very large openings connecting the inside and outside of the stator), and in the case when the size of the gap is 10 times that of the base line case (very large space between the tips of impeller blades and internal surface of stator). This means that the gap between the tips of impeller blades and internal surface of the stator acts as a sink of turbulent kinetic energy, strongly consuming the kinetic energy fed to the fluid by the agitation of the impeller. The more energy fed into the turbulent fluid flow, roughly the more turbulent kinetic energy is consumed inside this gap. Because the rotational speed of the of impeller is directly related to the energy input rate, it is reasonable to predict that low speed can lead to low turbulence dissipation rate and hence low characteristic shear rate.

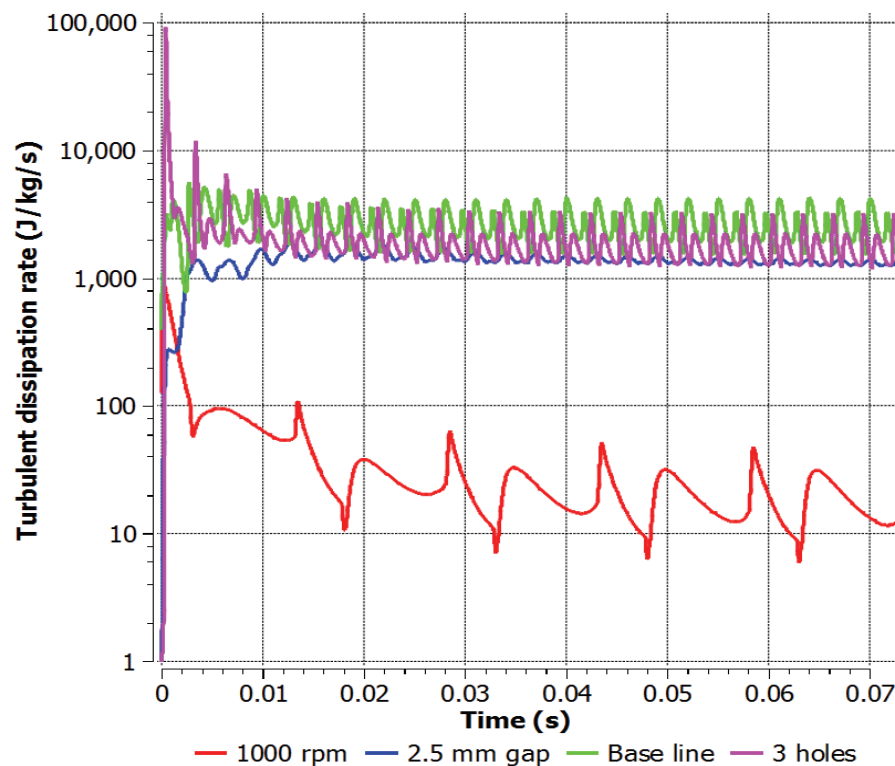


**Figure 7.** Temporal evolution of turbulence dissipation rate sampled at Point 1 with different setups.

In Fig.7, it is clear that the turbulence dissipation rate sampled at Point 1 in the 1000 rpm case is lower than those of the other cases by nearly 2 orders of magnitude. This directly supports our aforementioned theoretical analysis and we conclude that the energy input rate (related to impeller speed) dominates the performance of the mixing head in terms of refining the oxide clusters.

### Acknowledgement

This research is financially supported by the EC FP7 project “High Shear Processing of Recycled Aluminium Scrap for Manufacturing High Performance Aluminium Alloys” (Grant No. 603577).

### References

- [1] Li H, Wang Y and Fan Z 2012 Enhanced heterogeneous nucleation on oxides in Al alloys by intensive shearing *IOP Conf. Ser.: Mater. Sci. Eng.* **27** p 012047
- [2] Li H, Ji S, Wang Y, Xia M and Fan Z 2011 Effect of intensive melt shearing on the formation of Fe containing intermetallics in LM24 Al-alloy *IOP Conf. Series: Materials Science and Engineering* **27** p 012075
- [3] Peng G, Wang Y and Fan Z 2013 Effect of Intensive Melt Shearing and Zr Content on Grain Refinement of Mg-0.5Ca-xZr Alloys *Materials Science Forum* **765** pp 336-340
- [4] Patel J B, Prasada Rao A K, Jiang B, Zuo Y B, and Fan Z 2012 Melt Conditioned Direct chill casting (MC-DC) process for production of high quality Mg-alloy billets *Mg2012:9th International Conference on Magnesium Alloys and their Applications* pp 731-736
- [5] Xia M, Prasada Rao A K and Fan Z 2013 Solidification Mechanisms in Melt Conditioned Direct Chill (MC-DC) Cast AZ31 Billets *Materials Science Forum* **765** pp 291-295
- [6] Zuo Y B, Fan Z, Zhu Q F, Lei L and Cui J Z 2013 Modification of a Hypereutectic Aluminium Silicon Alloy under the Influence of Intensive Melt Shearing, *Materials Science Forum* **765** pp 140-144
- [7] Wang L, Marchisio D, Virgil R, Fox R 2005 CFD simulation of aggregation and breakage processes in laminar Taylor-Couette flow *Journal of Colloid and Interface Science* **282** pp 380-396
- [8] Yeoh G H, Cheung C, Tu J 2014 *Multiphase flow analysis using population balance modelling (bubbles, drops and particles)* Butterworth-Heinemann ISBN:978-0-08-0098229-8
- [9] Vanni M 2000 Creeping flow over spherical permeable aggregates *Chemical Engineering Science* **55** pp 685-698
- [10] Marchisio D, Vigil R, Fox R 2003 Implementation of the quadrature method of moments in CFD codes for aggregation-breakage problems *Chemical Engineering Science* **58** pp 3337-3351
- [11] Liao Y, Lucas D 2009 A literature review of theoretical models for drop and bubble breakup in turbulent dispersions *Chemical Engineering Science* **64** pp 3389 - 3406
- [12] Cheng J, Yang C, Mao Z, and Zhao C 2009 CFD Modeling of Nucleation, Growth, Aggregation, and Breakage in Continuous Precipitation of Barium Sulfate in a Stirred Tank *Ind. Eng. Chem. Res.* **48** pp 6992–7003
- [13] Maniruzzaman M D, Makhlof M M 2002 Mathematical Modeling and Computer Simulation of the Rotating Impeller Particle Flotation Process: Part II. Particle Agglomeration and Flotation *Mechanical Engineering Faculty Publications Department of Mechanical Engineering* 4-1-2002
- [14] Miroslav Soos, Rene Kaufmann, Raphael Winteler, Martin Kroupa, Beat Luthi 2013 Determination of Maximum Turbulent Energy Dissipation Rate generated by a Rushton Impeller through Large Eddy Simulation, *American Institute of Chemical Engineers* **59** pp 3642-3658